

Supporting Information

Polymerization of EDOT functionalized star shaped pentaerythritol and study of the structure and conducting properties of polymers.

Rana Abdel Samad, Frédéric Gohier, Barbara Daffos, Pierre-Louis Taberna and Charles Cougnon

Supporting Index

- 1. Instrumentations and Procedures**
- 2. Synthesis of EDOT functionalized pentaerythritol**
- 3. Electrochemical and chemical preparation of films**
- 4. FT-IT spectra of pentaerythritol-based monomer and polymer products**
- 5. Cyclic voltammetry study of films**
- 6. Brief digression on non-classical diffusion impedances**
- 7. References**

1. Instrumentations and Procedure

Electrochemical measurements were made in a three-electrode cell containing dichloromethane + 0.1 M nBu₄NPF₆. The counter electrode was a platinum wire and the working electrode was a glassy carbon electrode from Bioanalytical Systems Inc. (model MF-2012; 3 mm in diameter). The working electrode was mirror polished and sonicated for 5 min in DCM before analysis. All potential values were referred to the Ag/AgNO₃ system. A bipotentiostat from CH Instruments (model 920C) and a VMP-Biologic potentiostat (model SP-150) were used. Microgravimetric measurements were performed by using ATcut 9MHz gold-coated quartz crystal oscillators connected to a PAR quartz crystal analyser model QCM922 driven by the EC-Lab software (version 11.52). For impedance measurements, the amplitude of the ac signal was 5 mV and the frequency was varied between 500 kHz and 1 mHz.

Nitrogen adsorption–desorption isotherms were measured at 77K using Micromeritics ASAP 2020.

The Brunauer–Emmett–Teller (BET) equation was used to calculate the specific surface area (SSA). The pore size distribution (PSD) was calculated from adsorption isotherms using a 2D non-local density functional theory (2D-NLDFT) model based on Saeius software from Micromeritics.

FT-IR spectra were acquired with a resolution of 0.5 cm⁻¹ on a FT-IR Bruker Tensor 27 or a FT-IR VERTEX 70.

2. Synthesis of EDOT functionalized pentaerythritol

The EDOT functionalized pentaerythritol (compound 3 in Figure S1) was synthesized by copper(I)-catalyzed 1,3-dipolar cycloaddition (click chemistry) between 2-(azidomethyl)-2,3-dihydrothieno[3,4-b][1,4]dioxine (compound 1) and 3-(3-(prop-2-yn-1-yloxy)-2,2-bis((prop-2-yn-1-yloxy)methyl)propoxy)prop-1-yne (compound 2). Experimental protocols were described in detail for each compound, and proton and carbon NMR spectra were shown for compound 3.

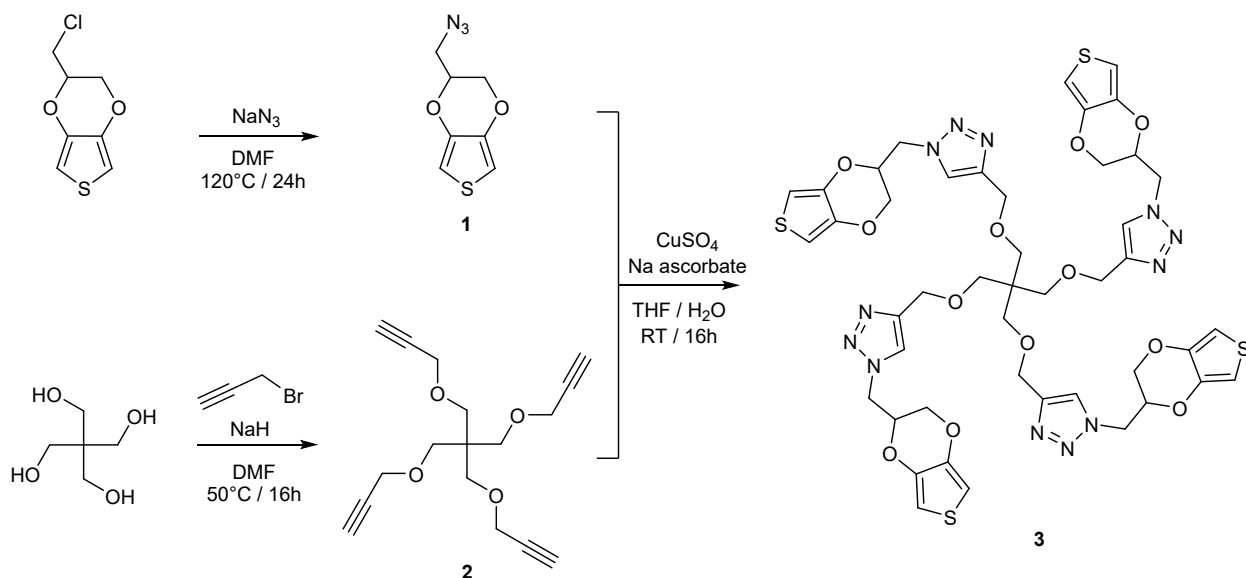


Figure S1: Synthesis strategy for the preparation of the EDOT functionalized pentaerythritol

2.1. Synthesis of compound 1: 2-(azidomethyl)-2,3-dihydrothieno[3,4-b][1,4]dioxine

This compound was synthesized according to a previously published procedure.¹ Chloromethyl-EDOT (1.00 g, 5.25 mmol, 1.00 eq.) was dissolved in anhydrous DMF (50 mL) under argon and NaN_3 (1.36 g, 21.00 mmol, 4.00 eq.) was added to this solution. The mixture was stirred for 24 h at 120°C. After cooling to room temperature, water was added (50 mL) and the solution was extracted with diethyl ether (3×50 mL) and washed with water (50 mL) and brine (3×25 mL). The organic layer was dried over anhydrous MgSO_4 and concentrated under reduced pressure to afford compound **1** (1.02 g, 99%) as a pale-yellow oil.

$^1\text{H NMR}$ (CDCl_3): δ 6.41 – 6.34 (m, 2H), 4.32 (m, 1H), 4.20 (dd, $J = 11.7, 2.3$ Hz, 1H), 4.05 (dd, $J = 11.7, 6.8$ Hz, 1H), 3.54 (qd, $J = 13.1, 5.6$ Hz, 2H).

2.2. Synthesis of compound 2: 3-(3-(prop-2-yn-1-yloxy)-2,2-bis((prop-2-yn-1-yloxy)methyl)propoxy)prop-1-yne

This compound was synthesized according to a previously published procedure.² A mixture of pentaerythritol (1.00 g, 7.35 mmol, 1.00 eq.) and NaH (1.57 g, 39.15 mmol, 5.33 eq., 60% w/w in mineral oil) was stirred at 0°C in anhydrous DMF (15 mL) under argon. After 30 min, propargyl bromide (4.28 mL, 40.01 mmol, 5.45 eq., 80% w/w in toluene) was added, and the mixture was heated at 50°C overnight. The reaction solution was poured into water and extracted with EtOAc. The combined organic layers were dried over MgSO_4 and concentrated under vacuo. The raw product was purified by silica gel column chromatography with DCM as eluent to give the desired compound (1.67 g, 79%) as a yellow-brown solid.

$^1\text{H NMR}$ (CDCl_3): δ 4.12 (d, $J = 2.4$ Hz, 8H), 3.53 (s, 8H), 2.40 (t, $J = 2.4$ Hz, 4H).

2.3. Synthesis of compound 3: 4,4'-(((2,2-bis(((1-((2,3-dihydrothieno[3,4-b][1,4]dioxin-2-yl)methyl)-1H-1,2,3-triazol-4-yl)methoxy)methyl)propane-1,3-diy)bis(oxy))bis(methylene))bis(1-((2,3-dihydrothieno[3,4-b][1,4]dioxin-2-yl)methyl)-1H-1,2,3-triazole)

A mixture of compound 2 (135 mg, 0.47 mmol, 1.00 eq.) and compound 1 (382 mg, 1.94 mmol, 4.10 eq.) was dissolved in THF (2 mL). $\text{CuSO}_4 \cdot 5\text{H}_2\text{O}$ (35 mg, 0.14 mmol, 0.30 eq.) in water (2 mL) and sodium ascorbate (56 mg, 0.28 mmol, 0.60 eq.) were added to the mixture and stirred overnight. The reaction solution was extracted with EtOAc and washed with water. The combined organic layers were dried over MgSO_4 and concentrated under vacuo. The product was purified by silica gel column chromatography with EtOAc and CH_3OH as eluents in a 9:1 volume ratio, to yield compound 3 as white powder (466 mg, 92%).

^1H NMR in CDCl_3 (Figure S2): δ 7.71 (s, 4H), 6.36 (q, $J = 3.6$ Hz, 8H), 4.64 (d, $J = 5.7$ Hz, 8H), 4.60 – 4.54 (m, 12H), 4.26 (dd, $J = 11.9, 2.2$ Hz, 4H), 3.94 – 3.84 (m, 4H), 3.47 (s, 8H).

^{13}C NMR in CDCl_3 (Figure S3): δ 145.7, 141.0, 140.4, 124.1, 100.8, 100.6, 72.0, 69.2, 65.6, 64.9, 50.0, 45.3.

HRMS calcd for $\text{C}_{45}\text{H}_{48}\text{N}_{12}\text{O}_{12}\text{NaS}_4$ ($[\text{M} + \text{Na}]^+$ ions): 1099.2289. Found: 1099.2275 (see Fig. S4).

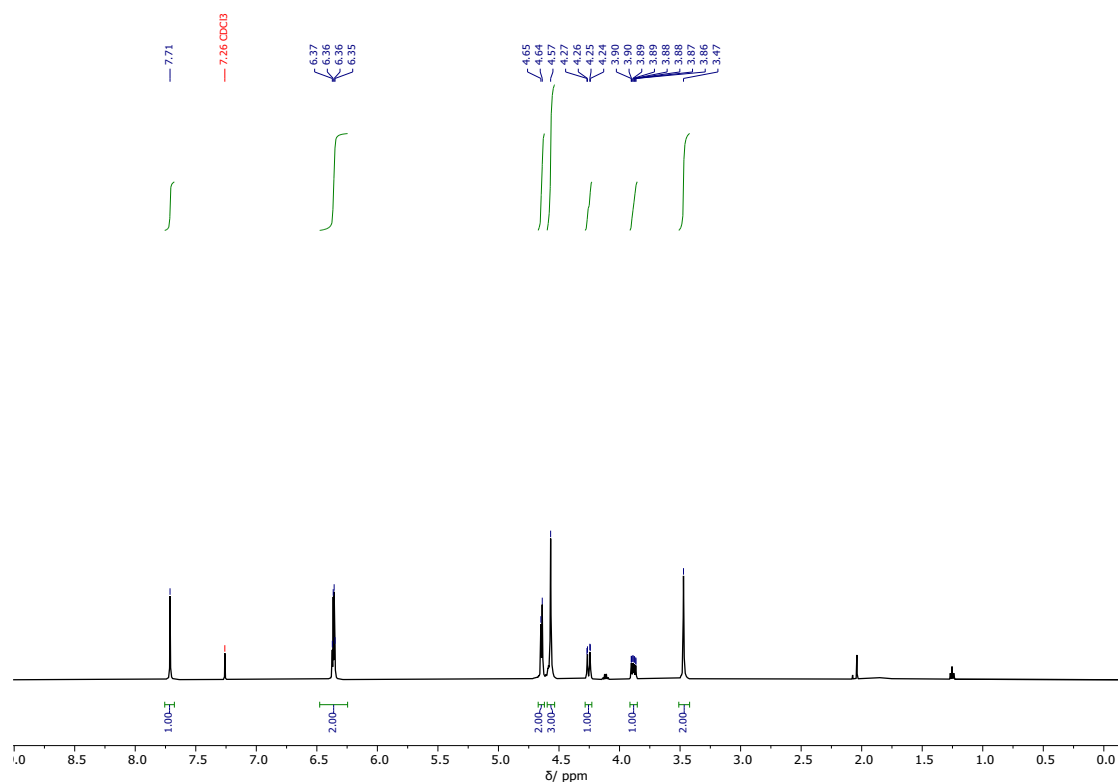


Figure S2: ^1H NMR spectrum of EDOT functionalized pentaerythritol in CDCl_3 solution.

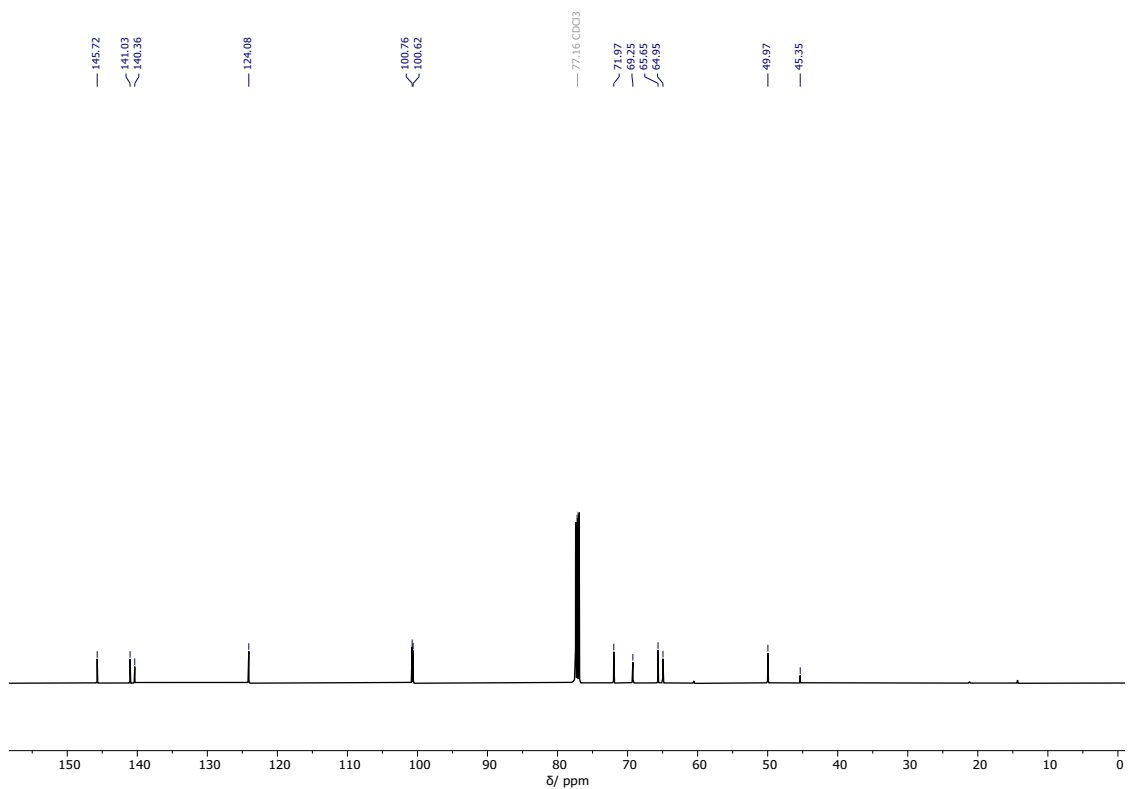


Figure S3: ^{13}C NMR spectrum of EDOT functionalized pentaerythritol in CDCl_3 solution.

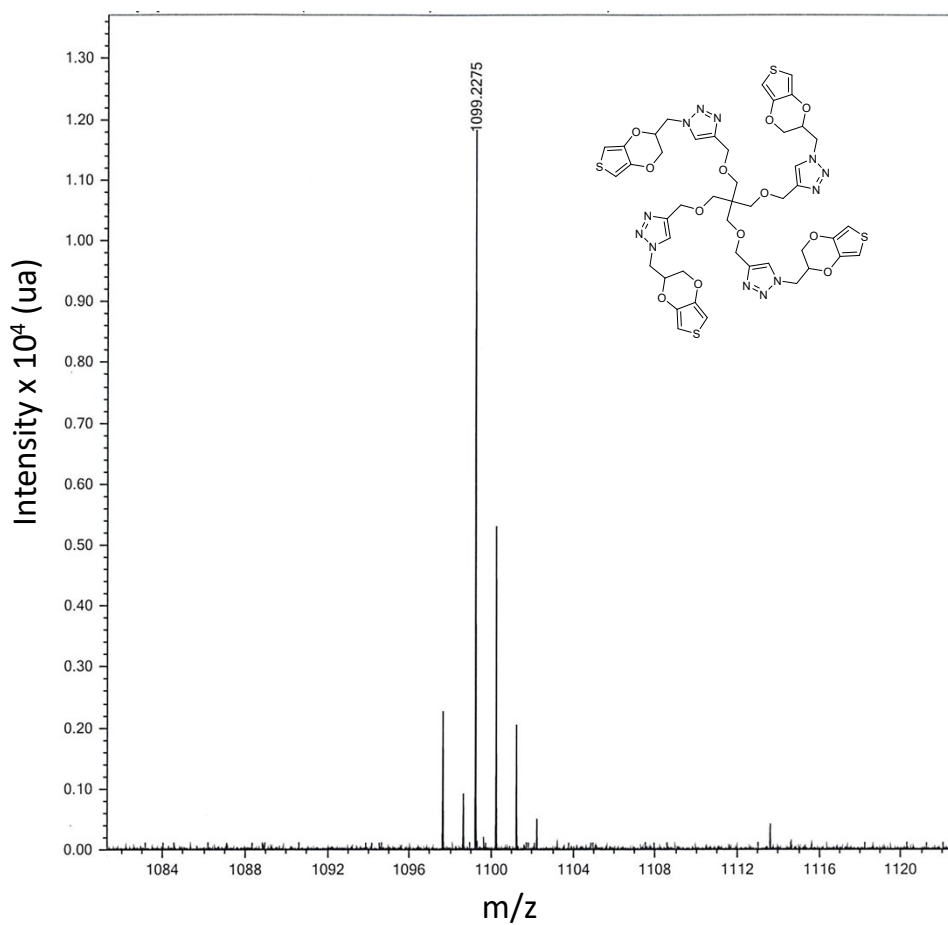


Figure S4: Mass spectrum of EDOT functionalized pentaerythritol

3. Electrochemical and chemical preparation of films

In the present work, polymers were prepared by electrochemical and chemical oxidation of monomers.³ For cyclic voltammetry, impedance and quartz crystal microbalance studies, polymers were prepared by electrochemical oxidation of monomers via cyclic voltammetry in DCM + 0.1 M Bu₄NPF₆. After formation on a glassy carbon electrode, films were studied in the same electrolyte free of monomers to avoid exchange of different solvents which would make more difficult the connection between free molecule of solvents and counter-anions exchange during the p-doping process. For cyclic voltammetry experiments, films were obtained in the neutral state by consuming an anodic charge close to 1 mC and studied in a glove box. For EIS experiments, films were obtained under the same conditions, but studied outside the glove box. For QCM experiments, the mass of films does not exceed 3000 ng to be sure that the Sauerbrey equation remains valid.

For nitrogen adsorption-desorption experiments, polymers were prepared by chemical oxidation of monomers because larger quantities of polymer were needed (typically comprised between 30 mg and 50 mg). For oxidative chemical polymerization, FeCl₃ was used as oxidant and films were obtained in their p-doped state (the anion of the chemical oxidant acting as counter anion to stabilize the p-doped polymer).^{4,5} Practically, FeCl₃ was used in excess with respect to the monomer with a FeCl₃/monomer molar ratio of 20, as the excess of oxidant is well known to be a key factor to promote the polymerization yield.⁶ The monomer was dissolved in deaerated DCM (0.05 mM or 0.5 mM) and slowly added in ACN containing FeCl₃. After complete addition, the solvent mixture of DCM/ACN (7:3, v/v) was stirred at room temperature for 48 h under argon. Then, the precipitate is filtered, washed with methanol to remove the oxidant in excess and dried under vacuum to give polymers as a black powder.

4. FT-IT spectra of pentaerythritol-based monomer and polymer products

FT-IR spectra of the synthesized EDOT-functionalized pentaerythritol monomer, PEDOT and pentaerythritol-based films were acquired to identify the main chemical functionalities in the polymer products as shown in Fig. S5. The vibrations at 1480 cm⁻¹, 1422 cm⁻¹, 1372 cm⁻¹ and 1344 cm⁻¹ originate from the stretching of C=C and C-C bonds in the thiophene ring.^{7,8} The characteristic peaks at 1224 cm⁻¹, 1184 cm⁻¹ and 1137 cm⁻¹ may be ascribed to the stretching vibration of the C-O-C bond in the ethylenedioxy bridge of the EDOT group.^{7,8} Vibrations from the C-S bond in the thiophene ring can be observed between 950 cm⁻¹ and 758 cm⁻¹.^{7,8} Vibrations at 1074 cm⁻¹, 1046 cm⁻¹ and 1014 cm⁻¹ can be ascribed to the stretching of the C-O bond of the pentaerythritol core.^{9,10} Noted that the peak at 1046 cm⁻¹ was also ascribed to the triazol structure.¹¹ With the same reasoning, the intense peak at 1480 cm⁻¹ can also be due to the stretching of the N=N bond in the triazol ring.¹² All of these characteristic bands allow to identify the main units (i.e. EDOT, triazol and pentaerythritol groups) in the EDOT-

functionalized-pentaerythritol-based film.

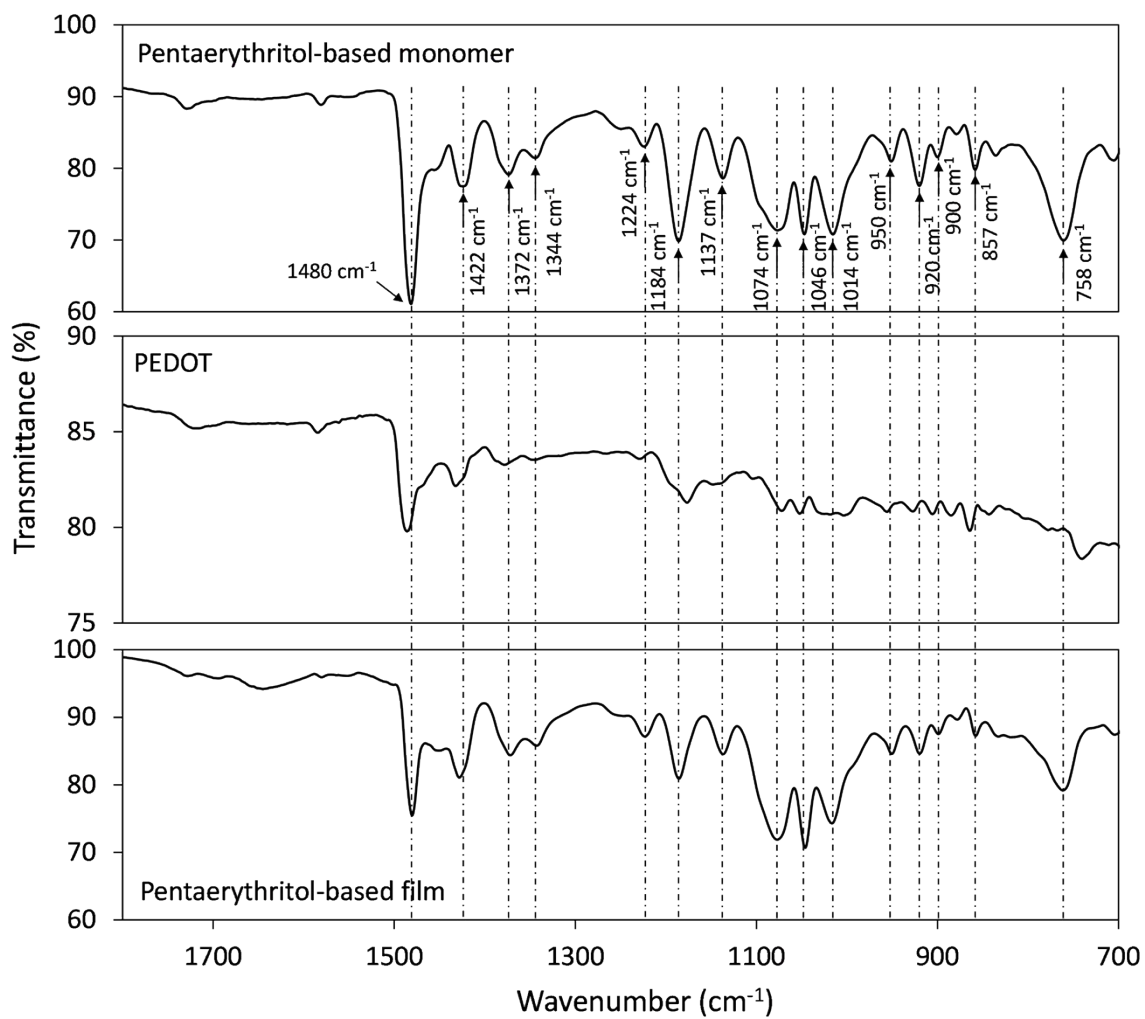


Figure S5: FT-IT spectra of pentaerythritol-based monomer, PEDOT and pentaerythritol-based polymer

5. Cyclic voltammetry study of films

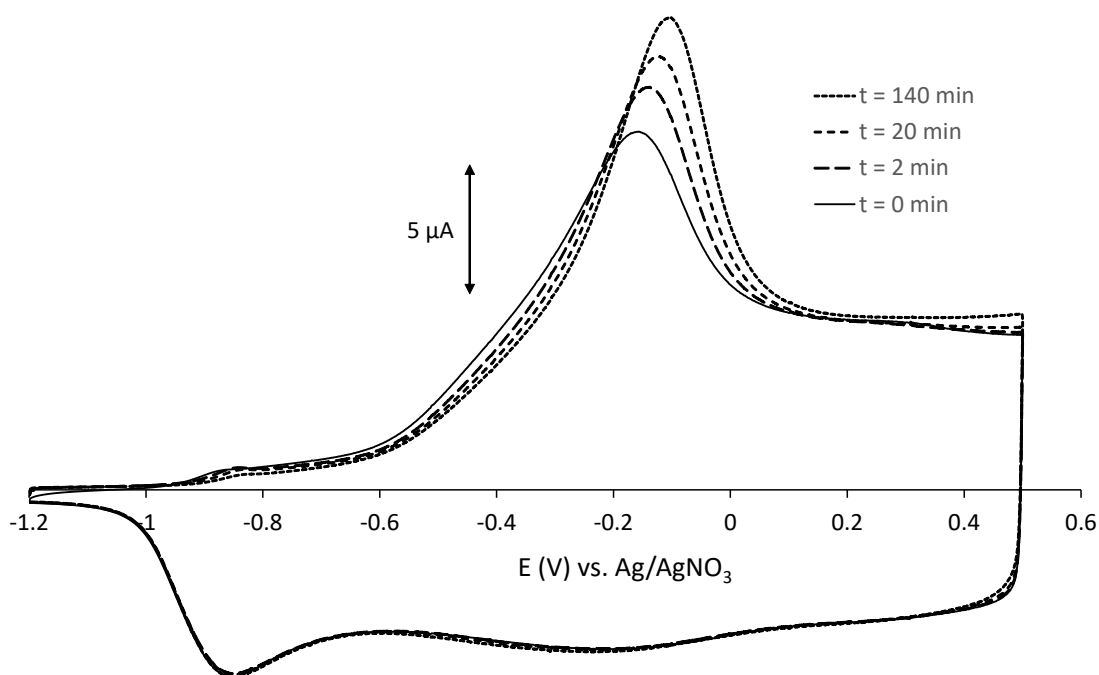


Figure S6: Cyclic voltammograms recorded at 50 mV s^{-1} in DCM + $0.1 \text{ M Bu}_4\text{NPF}_6$ on a GC electrode covered with a PEDOT film. In ascending order of the current peak intensity, the initial potential was set at -1.2 V for 0 min., 2 min., 10 min. and 140 min. before starting the CV. The PEDOT film was previously prepared by electrochemical oxidation of a 1 mM solution of EDOT in DCM + $0.1 \text{ M Bu}_4\text{NPF}_6$ by consuming a polymerization charge of 1.107 mC .

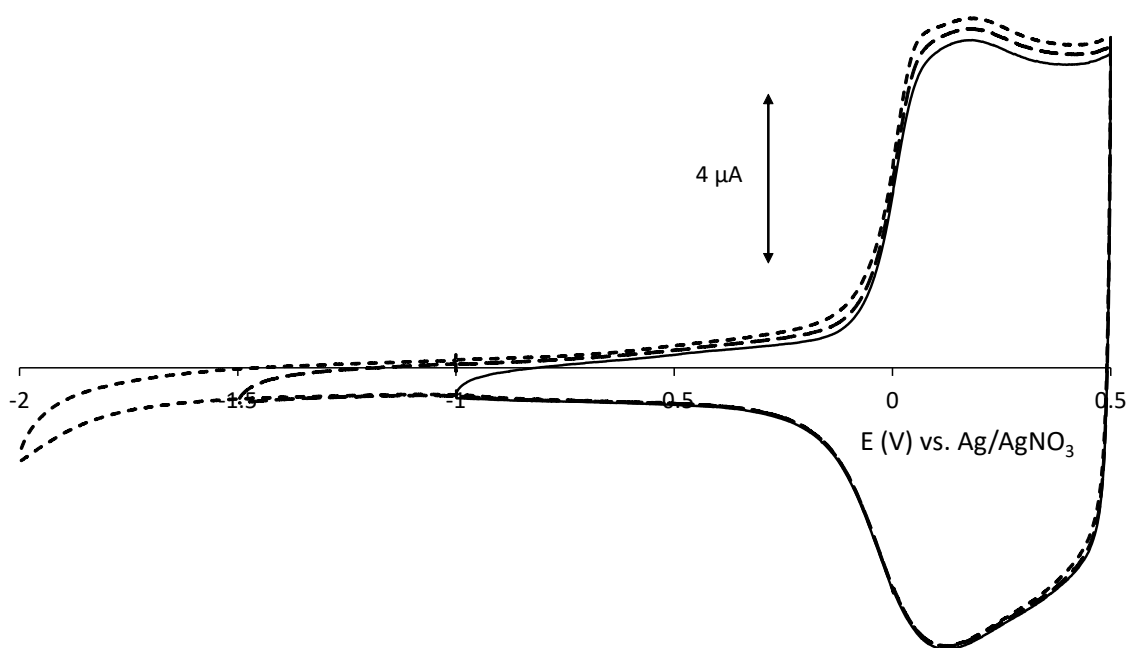


Figure S7: Cyclic voltammograms recorded at 50 mV s^{-1} in DCM + $0.1 \text{ M Bu}_4\text{NPF}_6$ by starting from different initial potentials on a GC electrode covered with a pentaerythritol-based film. The film was previously prepared by electrochemical oxidation of a 0.05 mM solution of EDOT functionalized pentaerythritol in DCM + $0.1 \text{ M Bu}_4\text{NPF}_6$ by consuming a polymerization charge of 1.05 mC .

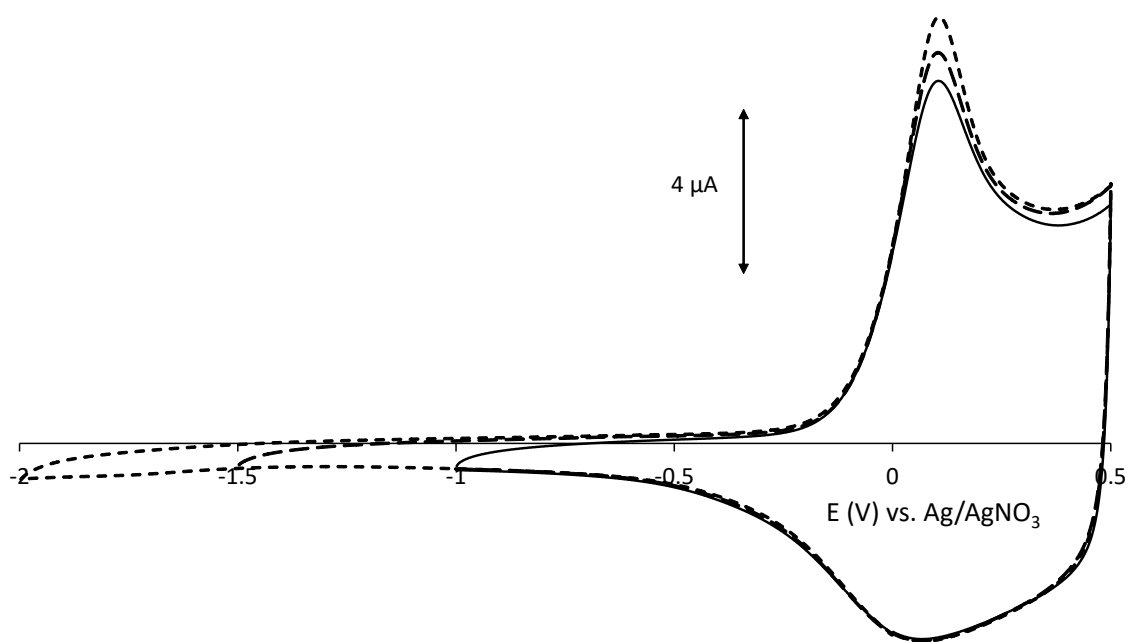


Figure S8: Cyclic voltammograms recorded at 50 mV s^{-1} in DCM + $0.1 \text{ M Bu}_4\text{NPF}_6$ by starting from different initial potentials on a GC electrode covered with a pentaerythritol-based film. The film was previously prepared by electrochemical oxidation of a 0.5 mM solution of EDOT functionalized pentaerythritol in DCM + $0.1 \text{ M Bu}_4\text{NPF}_6$ by consuming a polymerization charge of 1.05 mC .

6. Brief digression on non-classical diffusion impedance models

In literature, theoretical studies have shown that arced diffusion impedance may result to considerations about the boundary conditions for the mass transport at the electrode surface, depending on whether the electrode/film interface is considered as totally blocking (i.e. totally reflecting boundary condition), or permeable to ions (i.e. absorbing boundary condition). This aspect of the problem was discussed in detail by MacDonald, Jamnik and Maier and M.A. Vorotyntsev and M.D. Levi, using the continuum impedance model (Nernst-Planck-Poisson equations) concerned with two-charge-carrier conductors, such as mixed ion-electron-conducting polymers.¹³⁻¹⁵ In this model, charge carrier mobilities, concentrations and rate constants for ions and electrons may be responsible for deviation to the classical Warburg impedance. In the case of a not perfectly blocked electrode (envisioned as a non-zero rate constant for ions at the end of the diffusion zone), a “distortion” of the classical Warburg impedance in the low frequencies may result in a diffusion loop in the complex-plane impedance, as obtained in Figure 6 for the film prepared from the more concentrated monomer solution (solid circle symbols). Noted that non-zero rate constant for ions may also be envisioned as access to a reservoir when the diffusing species penetrates deeper in porous films.¹⁶ In the late 1990s, Bisquert et al. proposed a generalized boundary condition for the analytical treatment of spatially restricted diffusion impedance commonly referred to as the CPE-restricted diffusion model.^{17,18} In this model, the blocking boundary is designated as responsible for the diffusion impedance as a consequence of a complex coupling between the interfacial impedance and the diffusion impedance in the bulk of the film. The main idea is that above a critical frequency, the diffusion impedance does not

sense the boundary effects, retaining the classical Warburg response in the high frequency domain, while below the critical value, a complex coupling exists between surface and bulk impedances.¹⁹ Noted that the CPE-restricted diffusion model is well-suited for situations where a frequency dispersion is obtained at low frequencies and when the diffusion process obeys a Fickian behavior, which is the case for conducting polymers having a high electronic conductivity so that ions move across the film by diffusion or electromigration. However, in our situation, both the severe potential drop developed in the film and the transient nucleation phenomenon visible in Figure 5a are in conflict with the assumptions of the CPE-restricted diffusion model.

A more relevant model in place where a transient conduction regime occurs could be the model of anomalous diffusion that considers non-Fickian diffusion envisaged as diffusing tracers having a power law dependence on time for their mean squared displacement instead of a linear dependence.²⁰⁻²² In this model, the diffusion impedance deviates from a 45° line in the complex plane at high frequencies where the diffusion impedance senses the anomalous diffusion. The result is a straight line in the complex plane representation inclined at more or less than 45° according to the anomalous exponent and boundary conditions (the “normal” exponent 0.5 is quintessential for Fickian nature of the diffusion process in the canonical Warburg model). Although this is not in line with observations in the present work, we need to be careful with the conclusions drawn from these data because other specific situations than non-Fickian diffusion processes may give similar complex plane plots for the diffusion impedance, and because, the theoretical considerations in literature are based on a narrow windows of diffusion parameters and boundary conditions.

7. References

- 1 E. Scavetta, R. Mazzoni, F. Mariani, R. G. Margutta, A. Bonfiglio, M. Demelas, S. Fiorilli, M. Marzocchi, B. Fraboni, *J. Mater. Chem. B* **2014**, *2*, 2861.
- 2 G.-J. Liu, Y. Zhang, L. Zhou, L.-Y. Jia, G. Jiang, G.-W. Xing, S. Wang, *Chem. Commun.* **2019**, *55*, 9869.
- 3 S. Nie, Z. Li, Y. Yao, Y. Jin, *Front. Chem.* **2021**, *9*, 803509.
- 4 R. Corradi, S.P. Armes, *Synth. Met.* **1997**, *84*, 453.
- 5 Y. Jiang, T. Liu, Y. Zhou, *Adv. Funct. Mater.* **2020**, *30*, 2006213.
- 6 R.E. Myers, *J. Electron. Mater.* **1986**, *15*, 61.
- 7 C. Kvarnström, H. Neugebauer, S. Blomquist, H.J. Ahonen, J. Kankare, A. Ivaska, *Electrochim. Acta* **1999**, *44*, 2739.

- 8 B. Gupta, M. Mehta, A. Melvin, R. Kamalakannan, S. Dash, M. Kamruddin, A.K. Tyagi, *Mater. Chem. Phys.* **2014**, *147*, 867.
- 9 P. Ramamoorthy, N. Krishnamurthy, *Spectrochim. Acta A* **1997**, *53*, 655.
- 10 S. Akhan, B. Oktay, O.K. Özdemir, S. Madakbas, N.K. Apohan, *Mater. Chem. Phys.* **2020**, *254*, 123315.
- 11 A. Nagai, Y. Kamei, X.S. Wang, M. Omura, A. Sudo, H. Nishida, E. Kawamoto, T. Endo, *J. Polym. Sci. A: Polym. Chem.* **2008**, *46*, 2316.
- 12 E. Borello, A. Zecchina, E. Guglielminotti, *J. Chem. Soc. B*, **1969**, 307.
- 13 J. Jamnik, J. Maier, *J. Electrochem. Soc.* **1999**, *146*, 4183.
- 14 J.R. Macdonald, *Electrochim. Acta* **1992**, *37*, 1007.
- 15 M.A. Vorotyntsev, L.I. Daikhin, M.D. Levi, *J. Electroanal. Chem.* **1994**, *364*, 37.
- 16 S.J. Cooper, A. Bertei, D.P. Finegan, N.P. Brandon, *Electrochim. Acta* **2017**, *251*, 681.
- 17 J. Bisquert, G. Garcia-Belmonte, F. Fabregat-Santiago, P.R. Bueno, *J. Electroanal. Chem.* **1999**, *475*, 152.
- 18 J. Bisquert, G. Garcia-Belmonte, P. Bueno, E. Longo, L.O.S. Bulhões, *J. Electroanal. Chem.* **1998**, *452*, 229.
- 19 J. Bisquert, G. Garcia-Belmonte, F. Fabregat-Santiago, N.S. Ferriols, P. Bogdanoff, E.C. Pereira, *J. Phys. Chem. B* **2000**, *104*, 2287.
- 20 J. Bisquert, A. Compte, *J. Electroanal. Chem.* **2001**, *499*, 112.
- 21 J. Bisquert, G. Garcia-Belmonte, F. Fabregat-Santiago, A. Compte, *Electrochem. Commun.* **1999**, *1*, 429.
- 22 G. Garcia-Belmonte, J. Bisquert, E.C. Pereira, F. Fabregat-Santiago, *Appl. Phys. Lett.* **2001**, *78*, 1885.